




General Methodology to Investigate the Effect of Process Parameters on the Vibration Properties of Structures Produced by Additive Manufacturing Using Fused Filament Fabrication

FANGKAI XUE ^{1,2,3}, GUILLAUME ROBIN,¹ HAKIM BOUDAUD,²
FABIO A. CRUZ SANCHEZ,² and EL MOSTAFA DAYA¹

1.—LEM3, CNRS, Arts et Métiers ParisTech, Université de Lorraine, 57000 Metz, France.
2.—Equipe de Recherche sur les Processus Innovatifs (ERPI), Université de Lorraine, 54000 Nancy, France. 3.—e-mail: fangkai.xue@univ-lorraine.fr

Advances in fused filament fabrication (FFF) enable the manufacturing of multi-material and multi-functional structures, which provides new opportunities for the development of lightweight and high damping structures for vibration control. However, very few studies mention the vibration characteristics of FFF printed structures. This paper proposes a general methodology to investigate the effect of process parameters, such as raster angle, nozzle temperature, layer height, and deposition speed, on the vibration properties of FFF printed structures. An application of this methodology to structures printed by polylactic acid (PLA) is realized. In terms of vibration properties, a good reproducibility of the FFF process and the vibration test was achieved. It was found that raster angle significantly affects both resonant frequency (16.6%) and loss factor (7.5%). The impact of the other three parameters is relatively low (less than 4%). All these results provide guidance for further application of FFF in the vibration field.

INTRODUCTION

Fused filament fabrication (FFF), also known as fused deposition modeling (FDM) which is a trademark, is one of the most widespread additive manufacturing (AM) technologies. Various technical advancements of FFF have been achieved in recent decades, making it a more powerful and reliable technology.¹ At the material level, plenty of new materials have been developed for FFF such as metallic,² ceramic,³ fiber-reinforced polymers,⁴ and bio-polymers.⁵ At the machine level, recent developments in hybrid FFF⁶ and multi-material FFF⁷ provide a much wider space for the design and manufacturing of multi-functional structures. At the structural level, metamaterials and architecture structures with customized material properties have been realized via FFF.^{8,9}

All this progress enables FFF to be applied to more fields, and one of the trending areas is the use of FFF in vibration control. Some preliminary attempts have already been done. Compton and Lewis¹⁰ reported the extrusion-based 3D printing of lightweight cellular composites by a new epoxy-based ink with controlled alignment of multi-scale, high aspect ratio fiber reinforcement. Matlack et al.⁸ demonstrated the fabrication of a metamaterial for low-frequency and broadband vibration absorption with an FFF printed lattice and manually inserted steel cube damper. Mizukami et al.⁴ presented an FFF printed locally resonant carbon-fiber reinforced acoustic metamaterial for the attenuation of broadband vibration.

Despite the rapid progress, the application of FFF in vibration control is still in its infancy. One of the biggest obstacles is the lack of understanding of the effect of process parameters on the vibration properties of FFF printed structures, which is essential before implementing engineering structures with more complex vibration properties.

The process of FFF is controlled by many parameters which have a large impact on the final part's mechanical properties.^{11–15} Great efforts have been made to discover the relationship between the process parameters and the static mechanical properties of FFF printed parts, including tensile strength,¹¹ flexural strength,¹³ fracture,¹⁴ and fatigue.¹⁶ Rezayat et al.¹⁷ reported that a raster angle along the direction of load resulted in higher tensile strength because the bonding of polymer between adjacent filaments is not as strong as bonding of polymer within the filament. Goh et al.¹² demonstrated that greater layer height and higher printing speed result in a smaller degree of cooling and higher average temperature of the deposited filament, which can improve the interlayer fusion, and results in better mechanical properties in the across-the-layer direction.

However, only a few studies have mentioned the relationship between process parameters and the vibration properties of final parts. Seedhara et al.¹⁸ investigated the effect of build orientation and layer height on the modal properties of FFF printed ABS beams. They reported that the increase of layer height reduced the natural frequencies, and the specimen printed in a horizontal orientation had the highest natural frequencies. Raffic et al.¹⁹ studied the effect of infill density, layer height, and deposition speed on the natural frequency and resonant amplitude of FFF processed polyethylene terephthalate glycol-modified (PET-G) and acrylonitrile butadiene styrene (ABS) beams. Many other process parameters remain to be studied, and more in-depth analysis is needed to understand their mechanisms of influence.

Furthermore, in all former works, experiments were realized in a limited variation range of process parameters, which may lead to incomplete understanding of their influences. And a standard method to find the maximum variation range of parameters for printing does not exist. This paper, based on design of experiment (DoE), provides a general methodology to evaluate the effect of process parameters on the vibration properties of FFF printed structures within a large parameter variation range. Specifically, the effects of raster angle, nozzle temperature, layer height, and deposition speed on the vibration properties of FFF printed PLA structures were investigated. Firstly, to fully capture the effect of process parameters, their maximum variation ranges were identified by a full-factorial preliminary test. Then, the reproducibility of the proposed protocol was evaluated in terms of the measured vibration properties. Finally, the effect of these four key process parameters were investigated through DoE and modal analysis. All these results provide essential guidance for further application of FFF in the vibration field.

METHODOLOGY OF INVESTIGATION

A new methodology is proposed to evaluate the effect of process parameters on the vibration properties of FFF printed structures. It consists of three phases: (1) FFF setup and DoE, (2) experiment, and (3) results analysis (Fig. 1). With a full factorial pre-test built into this methodology, the effect of parameters can be investigated in a large variation range of parameters. This investigation protocol can be applied to structures printed with different FFF machines, materials, and geometries. In this research, an application case of PLA beams is demonstrated.

Phase I: Set-Up of FFF and DoE

In phase I, the material, machine, and geometry of the product, and the settings of process parameters are set up for FFF. To investigate the effect of process parameters, several key process parameters are selected for study through a literature review. Then, their variation ranges are determined through a full-factorial pre-test. The selected parameters and their variation ranges are used as factors and factor levels for DoE.

Material, Machine, and Geometry

FFF has a wide range of available materials.¹ The material used in this study was polylactic acid (Raise Premium 1.75 mm PLA filament), which is one of the most used materials in FFF, well known for its high stiffness, high strength, low melting point, non-toxic and non-irritation properties, and good biocompatibility.²⁰ These properties of PLA enlarge its potential application in vibration control. A commercial dual extruder FDM machine Raise 3D E2 was used for the fabrication. To investigate the flexural vibration modes, a beam specimen with a geometry of 3 mm thickness, 20 mm width and 200 mm length was chosen.

Selection of Key Process Parameters

Through a literature review, four process parameters and one of their interactions were selected as key parameters, and used as factors in DoE: raster angle (R); nozzle temperature (T); layer height (H); deposition speed (V); and interaction between raster angle and nozzle temperature (R–T). Raster angle has a severe effect on the mechanical resistance of a printed structure because of the anisotropic nature of the FFF process.¹¹ Nozzle temperature, layer height, and print speed control the thermal history of printing which dominates the bonding strength between filaments.¹² According to previous research, PLA has a high anisotropic property induced by the nature of the deposition process which makes the bond strength between filaments much weaker than the strength of deposited filaments.²¹ The raster angle can change the orientation of structure anisotropy by arranging the

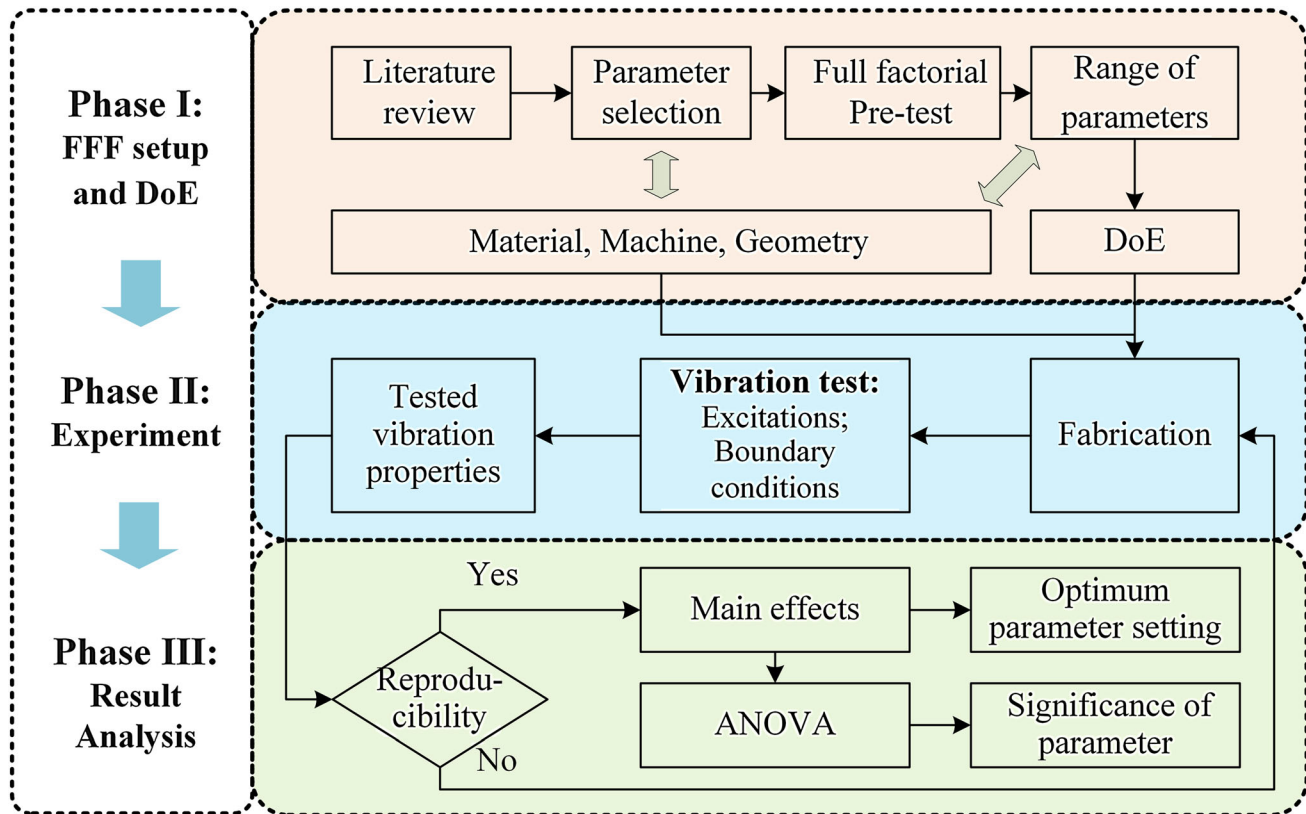


Fig. 1. Methodology of the experimental investigation.

direction of adjacent filament bonding. Meanwhile, the nozzle temperature influences the thermal history of printing and eventually controls the filament bonding strength. Therefore, it's supposed that there is an interaction between the raster angle and the nozzle temperature on the vibration properties of FFF structures.

Variation Ranges of Parameters for the Design of Experiment

A general challenge for DoE is the determination of the levels of factors. If the variation range of factors is too narrow, part of the influence of parameters will be missed during the experiment. On the other hand, if the variation range of factors is too wide, some test runs may fail during the experiment, leading to data loss for further analysis. Unfortunately, the boundary between the maximum and the excessive variation range of parameters is usually unknown before the experiment. In the literature, factor levels are usually determined based on previous studies or engineering experience. A more robust method is developed here.

In this study, a full-factorial pre-test is proposed to identify the maximum variation range of factors (Table I). The idea is to find out the boundary of this parameter space through a simpler and faster pre-test before the main test. Firstly, a full-factorial

DoE was developed to include all possible combinations of the levels of parameters. In the case of PLA, raster angle is considered to be a structural parameter which changes the orientation of discontinuity of the structure, but does not affect the print quality. Therefore, only nozzle temperature, layer height, and deposition speed were selected for the full factorial test. Values of other process parameters were pre-fixed as follows: build orientation, horizontal; extrusion width, 0.4mm; flow rate, 100%; bed temperature, 60°C; cooling, 100%; infill density, 100%; infill pattern, line.

Secondly, to economize the time of fabrication, a simplified beam specimen with a geometry of 1.2 mm thickness, 10 mm width, and 100 mm length was used for the full factorial DoE. It's assumed that the simplified beam can represent the printing quality of the beam specimen for the vibration test.

Next, the printing quality of specimens was verified by naked-eye observation. Three kinds of defects were considered as unacceptable for later vibration tests (Fig. 2). The first one was visible pores (Fig. 2a,b) which were observed at small layer height and high deposition speed. The second was discontinuous deposited filaments (Fig. 2c) observed at big layer height and high deposition speed. The third was the slippage of deposited filaments observed at low nozzle temperature, high deposition speed, and medium layer height (Fig. 2d). These three defects can heavily reduce the fatigue

Table I. Full factorial preliminary test of PLA beam

Parameter	T (°C)	180			190			200			220			250			260			
	H (mm)	0.1	0.2	0.3	0.1	0.2	0.3	0.1	0.2	0.3	0.1	0.2	0.3	0.1	0.2	0.3	0.1	0.2	0.3	
V (mm/s)	60				Selected test space															4
	70																			
	80			2																
	90																			
	100						2													
	110	1																		
	120				1					2										
	130		3																	
	140					1		1				2								
	150										1									
Defects	1. Visible pores; 2. Discontinuous deposited filament; 3. Slippage of deposited filaments; 4. Emission of harmful gas caused by thermal decomposition, may include: carbon oxides (CO, CO2), nitrogen oxides, HCN.																			

Acceptable printing quality

Selected test space

Critical conditions for the occur of unaccepted defects

Unacceptable printing quality

1,2,3,4

Type of unacceptable defects

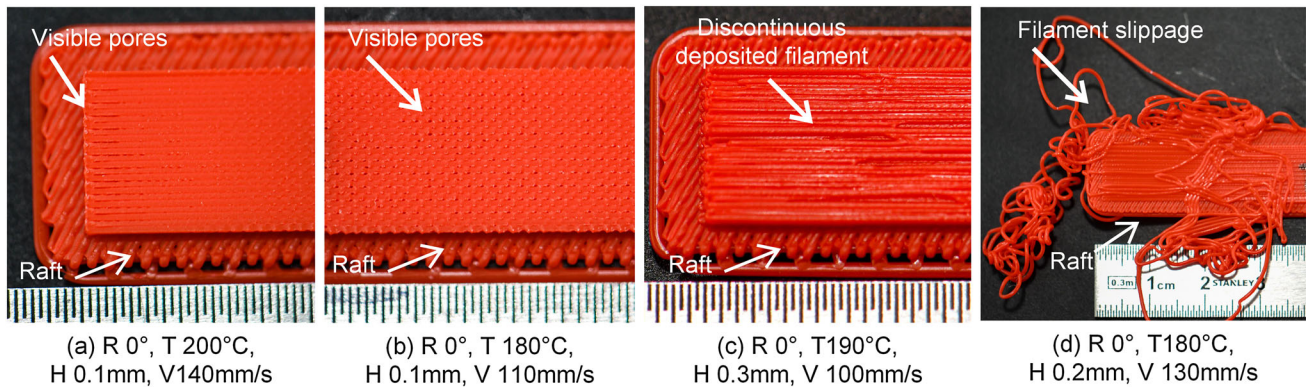


Fig. 2. Defects of specimens printed under critical conditions. (a) Visible pores at the end of specimen printed at small layer height and high deposition speed; (b) visible pores at the middle of specimen printed at small layer height, low nozzle temperature and high deposition speed; (c) discontinuous deposited filaments at big layer height and high deposition speed; (d) slippage of deposited filaments observed at low nozzle temperature, high deposition speed, and medium layer height.

resistance and the stiffness of specimens, which are important for vibration application. The fourth is the emission of harmful gas at temperatures excessively higher than the melting temperature (150°C for the selected PLA filament) of the material.²⁰ Finally, to capture the effect of parameters as completely as possible, a maximum available parameter space was selected for the DoE of the vibration test in the shaded area of Table I.

Design of Experiment in Use of Taguchi Method

In FFF, design of experiments (DoE) is widely used to reduce time costs and apply statistics to the experiment.²² One of the most used DoE methods in FFF is the Taguchi method because it strikes a balance between statistical analysis and operational simplicity.^{22,23}

Table II. Levels of factors for Taguchi design of PLA experiment

Levels	R (°)	T (°C)	H (mm)	V (mm/s)
1	0	190	0.1	20
2	90	220	0.2	55
3	/	250	0.3	90

According to the result of the preliminary test, the four selected key process parameters were used as the multi-level factors of Taguchi method (Table II). To include the effect of interaction between the raster angle and the nozzle temperature in the study, a Taguchi $L_{18}(2^1 3^3)$ orthogonal array was developed (Table III). T, H, and V have three factor

levels, while R only has two levels due to the statistical limitation of the Taguchi method. To obtain the maximum difference in stiffness and verify the maximum effect of parameters, 90° and 0° were chosen as the levels of raster angle.

Phase II: Experiment

Fabrication

A total of 36 specimens were printed according to the DoE in Table III. Each test trial had two

Table III. Taguchi $L18(2^1 3^3)$ orthogonal arrays for the DoE for PLA

Trials	Specimen	Replication	Factors				R-T
			R	T	H	V	
1	PLA 1111	2	1	1	1	1	(1,1)
2	PLA 1122	2	1	1	2	2	
3	PLA 1133	2	1	1	3	3	
4	PLA 1211	2	1	2	1	1	(1,2)
5	PLA 1222	2	1	2	2	2	
6	PLA 1233	2	1	2	3	3	
7	PLA 1312	2	1	3	1	2	(1,3)
8	PLA 1323	2	1	3	2	3	
9	PLA 1331	2	1	3	3	1	
10	PLA 2113	2	2	1	1	3	(2,1)
11	PLA 2121	2	2	1	2	1	
12	PLA 2132	2	2	1	3	2	
13	PLA 2212	2	2	2	1	2	(2,2)
14	PLA 2223	2	2	2	2	3	
15	PLA 2231	2	2	2	3	1	
16	PLA 2313	2	2	3	1	3	(2,3)
17	PLA 2321	2	2	3	2	1	
18	PLA 2332	2	2	3	3	2	

replications.

Vibration Test

Modal analysis was used to characterize the vibration properties of PLA beams (Fig. 3). The specimen was excited by a shaker controlled by a controller device (UCON system). The range of frequency excitation was between 10 Hz and 2000 Hz. To minimize nonlinear vibrations, a typical 1 mm of vibration amplitude and a 1 *g* acceleration were chosen for the excitation. The vibration amplitude of the shaker was measured by an accelerometer (PCB Piezotronics). The vibration amplitude of the beam was measured by a laser vibrometer. The response spectrum using frequency response function (FRF) data was used to determine the resonant frequencies and the loss factors through the half-power bandwidth method (HPBM, also known as the -3 dB method).

For PLA specimens, the boundary condition was clamped-free and the laser spot was pointed on the free extremity of the beam which could capture all vibration modes on the selected spectral. The beams were attached to the shaker by an apparatus with a clamp length of 15 mm.

Tested Vibration Properties

To establish a quantitative qualification, two vibration properties were selected as key indexes: resonant frequency and loss factors. Resonant frequency is a fundamental index of vibration in a frequency domain vibration test. Moreover, the damping of structures is very important for vibration control. And the loss factor is a common index used to characterize the damping of a material or structure, which is equal to the ratio between the loss modulus and the storage modulus.

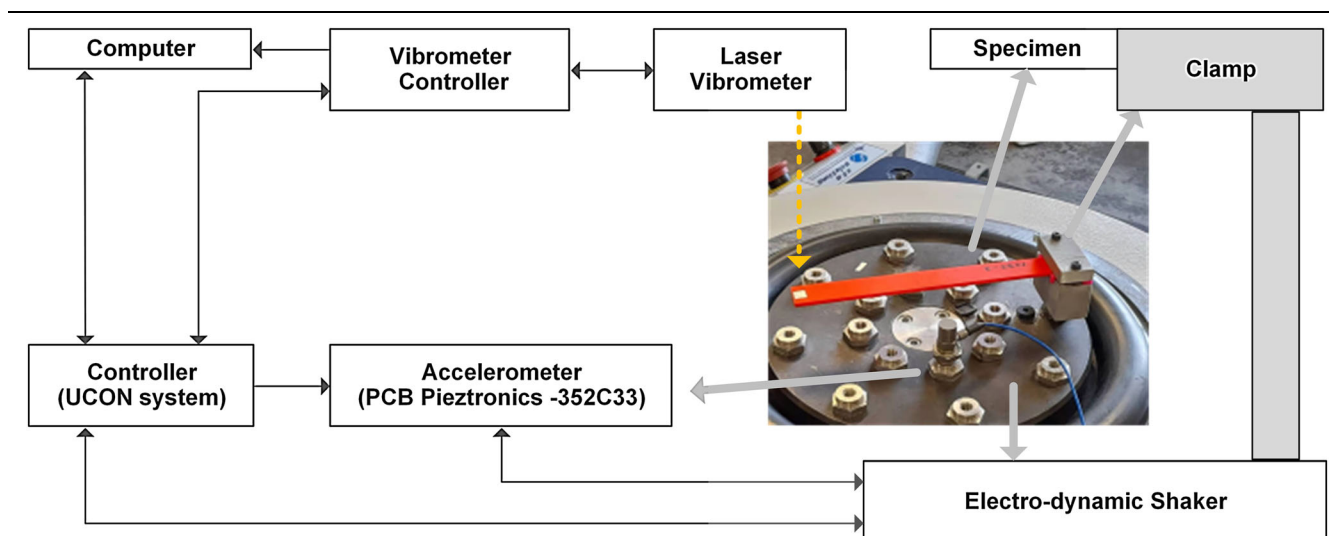


Fig. 3. Experiment setup for modal analysis.

Table IV. Reproducibility of FDM-printed PLA beam

Item	Mode 1	Mode 2	Mode 3	Mode 4	Mode 5
Resonant frequency (Hz)	21.97±0.12	135.77±1.02	379.52±2.45	744.56±4.77	1228.84±8.12
Percentage error (%)	0.57	0.75	0.65	0.65	0.67
Loss factor	0.0292±0.0004	0.0149±0.0008	0.0125±0.0007	0.0122±0.0007	0.0127±0.0006
Percentage error (%)	1.26	5.86	5.78	5.56	5.13

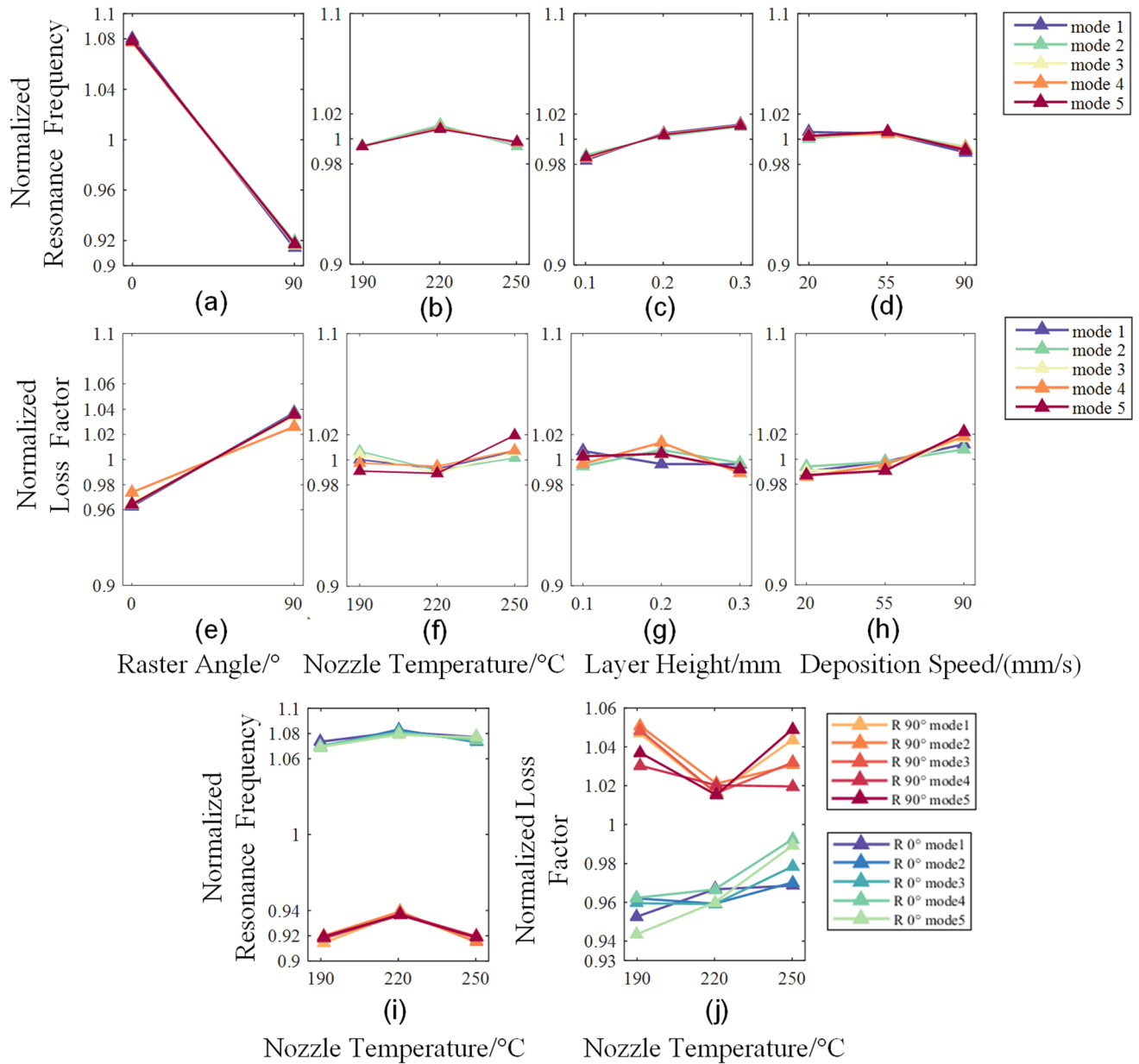


Fig. 4. Effect of (a) raster angle, (b) nozzle temperature, (c) layer height, and (d) deposition speed on the resonant frequency; effect of (e) raster angle (f) nozzle temperature, (g) layer height, and (h) deposition speed on the loss factor; effect of the interaction between raster angle and nozzle temperature on the (i) resonant frequency and the (j) loss factor.

RESULT AND DISCUSSION

Reproducibility Evaluation

To guarantee the reliability of the identified effects of parameters, the precision of the FFF process and the vibration test was evaluated in terms of the reproducibility of the measured vibration properties. A PLA beam with the same geometry as the vibration specimens was printed 6 times repetitively, at medium parameter levels as follows: R, 0°; T, 220°C; H, 0.2 mm; V, 55 mm/s.

The results of resonant frequencies show a high-level reproducibility with a percentage error smaller than 1% (Table IV). The percentage error is the ratio between the standard deviation and the average value. On the other hand, the percentage errors of loss factors are much higher than those of resonant frequencies, but still good (smaller than 6%). That is because the damping of PLA is relatively low. Therefore, the value of loss factors is too small to be precisely measured. Overall, this high reproducibility verifies the precision and the reliability of the fabrication and vibration test, laying a solid foundation for further identification of the effects of parameters.

Main Effects on the Resonant Frequency of PLA Beams

Through modal analysis, five resonant modes of the PLA beam were obtained (Fig. 4). Since the resonant frequency of each mode varied from 20 Hz to 1500 Hz, the main effects of parameters on the resonant frequency were normalized by the average resonant frequency of all specimens in each mode, to make a comparable analysis. Similarly, the main effects of loss factors were normalized by the average loss factor of all specimens in each mode.

Considering the raster angle, from 90° to 0°, the resonant frequencies decrease by 16.6% (Fig. 4a). This shows that PLA has a high anisotropic property in terms of resonant frequency, which is consistent with the reported anisotropy^{24,25} in static mechanical properties. A raster angle perpendicular to the axis of vibration form (axial axis for flexural vibration mode) leads to a larger resonant frequency as well as higher stiffness.

Nozzle temperature shows a nonlinear behavior where the resonant frequency increases by 1.6% from 190°C to 220°C, then decreases by 1.3% from 220°C to 250°C (Fig. 4b). The increase of resonant frequency from low temperature to middle temperature is due to the improvement of bonding degree between filaments. A higher average temperature can improve the inter-molecular diffusion between filaments which leads to better bonding strength. However, an excessively high temperature will cause radical degradation²⁰ of material. This is the cause of the decrease of resonant frequency from middle temperature to high temperature level, where the high temperature level (250°C) is 100°C

higher than the melting temperature of PLA (150°C).

Resonant frequency increases with the increase of layer height (Fig. 4c). From 0.1 mm to 0.2 mm, the resonant frequency increases by 2.2%; from 0.2 mm to 0.3 mm, the resonant frequency increases by 0.7%. As layer height increases, fewer numbers of layers need to be deposited, resulting in fewer thermal cycles and a smaller thermal gradient during printing, which was reported to have a positive effect on adhesion strength between filaments,¹² thus leading to higher stiffness and higher resonant frequency.

For deposition speed, the resonant frequency remains at the same level (0.7% of variation) as the deposition speed increases from 20 mm/s to 55 mm/s, and decreases by 1.5% as deposition speed increases from 55 mm/s to 90 mm/s (Fig. 4d). A higher deposition speed leads to less time for bonding formation between filaments and smaller necks.

The effect of interaction between raster angle and nozzle temperature on the resonant frequency is shown in Fig. 4i. The effect of nozzle temperature shows the same trends on all levels of layer height but is more important at a higher level of raster angle. At 0°, resonant frequency increases by 0.8% as nozzle temperature increases from 190°C to 220°C, then decreases by 0.4% as nozzle temperature increases from 220°C to 250°C. This effect is very weak and is at the same level of measurement deviation as that assessed in the reproducibility test. At 90°, the resonant frequency increases by 2.3% as nozzle temperature increases from 190°C to 220°C, then decreases by 2.2% as nozzle temperature increases from 220°C to 250°C, which is more significant than the effect of nozzle temperature at 0°. That's because the vibration of the beam is in flexural mode. Thus, at 90°, the direction of filament bond is parallel to the axis of flexural mode and contributes more to the global flexural modulus of the beam. This interaction shows that filament bond strength plays a more important role in vibration when the raster angle is parallel to the axis of vibration mode.

For the resonant frequencies of PLA beams, the following insights were retrieved:

- Raster angle has the most significant effect on the resonant frequency of the PLA beam;
- Effects of nozzle temperature, layer height, and deposition speed are relatively low;
- Effects of parameters show a consistent impact in all five resonant modes.

Main Effects on the Loss Factors of PLA Beams

Since the variation in loss factors for each mode is very similar, the following quantitative descriptions will be based on the first resonant mode. Raster

Table V. Significance of parameters on the resonant frequency of PLA beams

Source	Sum Sq.	d.f.	Mean Sq.	F	Prob>F	Signif	Contribution (%)
R	116.07	1	116.07	365.80	7.74E-17	***	89.34
T	0.90	2	0.45	1.42	0.26		0.21
H	2.97	2	1.49	4.68	0.02	*	1.80
V	1.06	2	0.53	1.67	0.21		0.33
R*T	0.31	2	0.16	0.49	0.62		- 0.25
Error	8.25	26	0.32				8.57
Total	129.56	35					100.00

Signif. codes: 0 < *** < 0.001 < ** < 0.01 < * < 0.05.

Table VI. Significance of parameters on the loss factor of PLA beams

Source	Sum Sq.	d.f.	Mean Sq.	F	Prob>F	Signif	Contribution (%)
R	4.20E-05	1	4.20E-05	52.97	9.93E-08	***	59.66
T	9.44E-07	2	4.72E-07	0.59	0.56		- 0.93
H	7.45E-07	2	3.72E-07	0.47	0.63		- 1.22
V	2.49E-06	2	1.24E-06	1.57	0.23		1.30
R*T	2.29E-06	2	1.14E-06	1.44	0.25		1.01
Error	2.06E-05	26	7.93E-07				40.17
Total	6.91E-05	35					100.00

Signif. codes: 0 < *** < 0.001 < ** < 0.01 < * < 0.05.

angle has the most significant influence on the loss factor of PLA beams (Fig. 4e). From 0° to 90°, loss factors reduce by 7.5%. Regarding nozzle temperature, the loss factor drops by 0.7% from 190°C to 220°C and increases by 1.4% from 220°C to 250°C (Fig. 4f). For deposition speed, the loss factor increases by 0.8% from 20 mm/s to 50 mm/s, then increases by 1.4% from 55 mm/s to 90 mm/s (Fig. 4h).

For the loss factors of PLA beams, the following insights are retrieved:

- Values of loss factors are very small which indicates that the damping capacity of PLA beams is very low;
- The raster angle has a significant effect on the loss factors of PLA beams, while the effects of nozzle temperature, layer height, and raster angle are relatively weak;
- Except for layer height, parameters show a consistent impact on all five resonant modes;
- Except for the layer height, the effect of each parameter on the loss factors shows an inverse trend to its effect on the resonant frequencies.

Analysis of Variance

In order to provide a correct interpretation of the effect of factors, an ANOVA analysis is necessary. This provides a significance rating of the relative influence of each factor analyzed in this study. Percentage contributions of each parameter on the response of specimens were also calculated.

Since the results of the ANOVA were consistent for all five resonant modes of PLA beams, only the result of the first mode, which is the most important for vibration control, is presented. Considering the effect on resonant frequency (contribution: 89.34%), the result of the ANOVA shows that raster angle is the most significant parameter, followed by layer height (Table V).

Considering the effect on the loss factor (Table VI), the raster angle is the only significant parameter, but it should be noted that there are large residual errors (contribution: 40.17%). There can be two sources for this residual error: (1) variable process parameters not considered in fabrication; and (2) noise of measurement in modal analysis. If the main cause is the first one, the residual errors for the resonant frequency should have a similar value compared to that of loss factor, which is not true. Therefore, this unusual residual error is mainly caused by the noisy measurement of loss factors in

modal analysis because small values of loss factors make the noise of measurement much more important.

CONCLUSION AND PERSPECTIVE

The use of FFF for the manufacturing of functional parts requires in-depth study on the vibration properties of FFF printed structures to prevent unwanted dynamic damage. In the absence of related studies on the relationship between process parameters and the vibration properties of printed parts in the literature, this study proposes a general methodology based on design of experiment (DoE), to evaluate the effect of process parameters on the vibration properties of FFF printed structures. Due to the built-in DoEs, the effect of parameters within a large parameter variation range can be investigated by a reduced number of tests.

As a case study, the effect of four process parameters, raster angle, nozzle temperature, layer height, and deposition speed, on the vibration properties of FFF printed PLA beams was investigated using modal analysis and DoE. The proposed methodology combined with a full factorial pre-test and Taguchi method ensures the success of the experiment in the identified maximum variation range of parameters. A high reproducibility (percentage errors smaller than 1%) was obtained in terms of resonant frequency in selected parameter levels. With a constant printing quality, FFF printed PLA parts are suitable for use as rigid components to reinforce the stiffness of structures and prevent vibration at low frequency. The following guidelines are summarized for the optimization of the vibration properties of FFF printed PLA structures:

1. The raster angle has the largest effect on both resonant frequency (16.6% of variation) and loss factors (7.5% of variation). A raster angle perpendicular to the axis of vibration form (axial axis for flexural vibration mode) leads to a higher stiffness as well as higher resonant frequency.
2. The effect of layer height on the resonant frequency is much smaller than that of raster angle but is still significant. A larger layer height leads to higher resonant frequency as the adhesion strength between filaments is improved by the reduction of thermal cycles and thermal gradient.
3. The effects of nozzle temperature, deposition speed, and the interaction between raster angle and nozzle temperature on the resonant frequency are also observed in the experiment but are not statistically significant. Therefore, a constant manufacturing quality can be achieved within the selected range of nozzle temperatures and deposition speeds in terms of vibration properties.

It should be mentioned that the importance and influence of process parameters of different materials may be different. Therefore, future research should focus on materials different from PLA, such as elastomers, ceramics, and metals. The reproducibility of FFF process in terms of vibration properties should also be verified on different materials and geometries.

ACKNOWLEDGEMENTS

The French Ministry of Research (DRRT), the regional Council "Région Lorraine", and the European Regional Development Fund (FEDER) has contributed to the funding of the vibration and wave propagation platform. Also, the authors would like to thank to the research platform Lorraine Fab Living Lab® for technical assistance in this research.

CONFLICT OF INTEREST

The authors declare that they have no conflict of interest.

REFERENCES

1. S. Singh, G. Singh, C. Prakash, and S. Ramakrishna, *J. Manuf. Process.* 55, 288 (2020).
2. S.H. Masood, and W.Q. Song, *Assem. Autom.* 25, 309 (2005).
3. S. Singh, S. Ramakrishna, and R. Singh, *J. Manuf. Process.* 25, 185 (2017).
4. K. Mizukami, T. Kawaguchi, K. Ogi, and Y. Koga, *Compos. Struct.* 255, 112949 (2021).
5. H. Chim, D.W. Hutmacher, A.M. Chou, A.L. Oliveira, R.L. Reis, T.C. Lim, and J.-T. Schantz, *Int. J. Oral Maxillofac. Surg.* 35, 928 (2006).
6. D. Grguraš, and D. Kramar, *Stroj. Vestn. – J. Mech. Eng.* 63, 567 (2017).
7. D. Espalin, J. Alberto Ramirez, F. Medina, and R. Wicker, *Rapid Prototyp. J.* 20, 236 (2014).
8. K.H. Matlack, A. Bauhofer, S. Krödel, A. Palermo, and C. Daraio, *Proc. Natl. Acad. Sci.* 113, 8386 (2016).
9. T. Jiang, C. Li, Q. He, and Z.-K. Peng, *Nat. Commun.* 11, 2353 (2020).
10. B.G. Compton, and J.A. Lewis, *Adv. Mater.* 26, 5930 (2014).
11. T.J. Gordelier, P.R. Thies, L. Turner, and L. Johanning, *Rapid Prototyp. J.* 25, 19 (2019).
12. G.D. Goh, Y.L. Yap, H.K.J. Tan, S.L. Sing, G.L. Goh, and W.Y. Yeong, *Crit. Rev. Solid State Mater. Sci.* 45, 113 (2020).
13. O. Luzanin, V. Guduric, I. Ristic, and S. Muhic, *Rapid Prototyp. J.* 23, 1088 (2017).
14. N. Suksangpanya, N.A. Yaraghi, R.B. Pipes, D. Kisailus, and P. Zavattieri, *Int. J. Solids Struct.* 150, 83 (2018).
15. F.A.C. Sanchez, H. Boudaoud, L. Muller, and M. Camargo, *Virtual Phys. Prototyp.* 9, 151 (2014).
16. V. Shanmugam, O. Das, K. Babu, U. Marimuthu, A. Veerasimman, D.J. Johnson, R.E. Neisiany, M.S. Hedenqvist, S. Ramakrishna, and F. Berto, *Int. J. Fatigue* 143, 106007 (2021).
17. H. Rezayat, W. Zhou, A. Siriruk, D. Penumadu, and S.S. Babu, *Mater. Sci. Technol.* 31, 895 (2015).
18. K. Sreedhara, K. Reddy, and S.N.S.H. Ch, *Int. J. Innov. Res. Sci. Eng. Technol.* 3297, 4602 (2015).
19. N.M. Raffic, *Int. J. Mech. Prod. Eng.* 3, 28 (2017).
20. F. Carrasco, P. Pagès, J. Gámez-Pérez, O.O. Santana, and M.L. Maspoch, *Polym. Degrad. Stab.* 95, 116 (2010).
21. S.H. Ahn, C. Baek, S. Lee, and I.S. Ahn, *Int. J. Mod. Phys. B* 17, 1510 (2003).

22. D. Popescu, A. Zapciu, C. Amza, F. Baci, and R. Marinescu, *Polym. Test.* 69, 157 (2018).
23. N. Logothetis, *Qual. Reliab. Eng. Int.* 6, 195 (1990).
24. S. Ahn, M. Montero, D. Odell, S. Roundy, and P.K. Wright, *Rapid Prototyp. J.* 8, 248 (2002).
25. C. Ziemian, M. Sharma, and S. Ziemi, in *Mechanical Engineering*, ed. by M. Gokcek (InTech, 2012).

Publisher's Note Springer Nature remains neutral with regard to jurisdictional claims in published maps and institutional affiliations.